Eur. Phys. J. A **22**, 495–502 (2004)
DOI 10.1140/epja/i2003-10239-3

THE EUROPEAN PHYSICAL JOURNAL A

The η^3He scattering length revisited

A. Sibirtsev[1,a], J. Haidenbauer[1], C. Hanhart[1], and J.A. Niskanen[2]

[1] Institut für Kernphysik, Forschungszentrum Jülich, D-52425 Jülich, Germany
[2] Department of Physical Sciences, P.O. Box 64, FIN-00014 University of Helsinki, Helsinki, Finland

Received: 10 November 2003 / Revised version: 19 May 2004 /
Published online: 11 November 2004 –
Communicated by V. Vento

Abstract. The possible existence of η-mesic nuclei poses an interesting and still open issue of research. Since the occurence of such η-nucleus bound states is reflected in the corresponding η-nucleus scattering length, we critically review the present knowledge for the η^3He system. Specifically, we scrutinize the available experimental information for the reaction $p + d \to \eta + {}^3$He which is commonly used to extract the η^3He scattering length. We point out several striking discrepancies between the various measurements. Subject to those inconsistencies, we deduce a value $a = |4.3 \pm 0.3| + i(0.5 \pm 0.5)$ fm.

PACS. 21.45.+v Few-body systems – 14.40.Aq Π, K, and η mesons – 11.80.Fv Approximations (eikonal approximation, variational principles, etc.) – 36.10.Gv Mesonic atoms and molecules, hyperonic atoms and molecules

1 Introduction

The possible formation of η-nucleus quasibound states has been an interesting topic for a long time. However, so far no such states have been directly observed. It is also an open and heavily debated question what might be the lightest nuclei for which such a bound state can occur. For instance, investigations [1–3] based on optical models indicate carbon as the lower limit for nuclei able to bind an η-meson. Most recently [4] this limit was lowered to the ^{4}He nucleus. In contrast, even formation of a bound η^3He system is supported by other and different model calculations [5–9]. To clarify the situation, experimental studies of this system are proposed at GSI [10,11] and COSY [12–14]. It is obvious that such experiments are very delicate and their design requires good estimates for the relevant binding energies and widths of η-mesic nuclei. Such estimates would dictate, for instance, the necessary resolution of the detector and the required beam luminosity.

In this context very light nuclei are particularly interesting because such systems are accessible to a microscopic treatment, whereas for heavier systems approximations have to be introduced whose effects are difficult to quantify and, accordingly, might lead to large uncertainties in the achieved results. In particular the η^3He system is very appealing because it can be studied within the well-established Alt-Grassberger-Sandhas [15] and Faddeev-Yakubovsky [16] theories. The only but still very crucial ambiguity here is caused by our poor knowledge of the elementary η-nucleon (ηN) interaction, which obviously enters any microscopic calculation as an input. A compilation of values for the ηN scattering length, obtained from different ηN model analyses, shows that its real part ranges from 0.20 to 1.05 fm, while the imaginary part varies between 0.16 and 0.49 fm [17]. Since the elementary ηN interaction is not fixed, any η-nucleus calculation [5–9] can only provide a range of results for the η-nucleus scattering lengths rather than a concrete prediction.

Under these circumstances it seems to be more promising to investigate a quantity closely related to the properties of the bound state, namely the η-nucleus scattering length [18]. It is well-known that in case of bound states the (real part of the) scattering length should be relatively large and negative. (We adopt here the sign convention of Goldberger and Watson [19] common in meson physics.) Thus, studies of the η-nucleus interaction near threshold can be used to determine the η-nucleus scattering length, and then, in turn, would permit conclusions on the existence of such η-nucleus bound states. Information on the η-nucleus interaction can be deduced from analysing the energy dependence of η production reactions such as $pd \to \eta^3$He, $dd \to \eta^4$He, etc. Certainly, the energy dependence of the production cross-section of those reactions itself is not sensitive to the sign of the real part of the scattering length, but only to its magnitude, and therefore cannot provide direct evidence for the existence of a bound state. (See, however, ref. [20] for a possible experiment to determine the sign of the real part.) But even a

[a] e-mail: a.sibirtsev@fz-juelich.de

good quantitative knowledge of the magnitude of the scattering length could already provide a strong hint for the existence of a η-mesic bound state and, more importantly, it would allow concrete estimations for the energy range that should be scanned in dedicated experiments.

In the present paper we provide a systematic overview of the experimental information available for the reaction $p + d \to {}^3\mathrm{He} + \eta$ [21–27]. In particular, we critically compare the results of the various measurements, which were partly performed for different kinematical conditions, in order to investigate the consistency of the data sets. Special emphasis will be put on the data near the reaction threshold which are commonly used to extract information about the η^3He scattering length. We discuss also results for the η^3He scattering length that can be found in the literature. The aim of the paper is twofold. First we want to derive a new estimate for the η^3He scattering length taking into account all available low-energy data on the reaction $p+d \to {}^3\mathrm{He}+\eta$ and, secondly, we want to specify which further measurements are necessary in order to significantly improve the present situation.

2 Treatment of the final-state interaction

If a production reaction is governed by a strong s-wave interaction in the final state then, according to Watson and Migdal [28,29], the energy dependence of the reaction amplitude is basically determined by the on-shell scattering amplitude of the final state, *i.e.* by

$$T(q) = \frac{1}{q\cot\delta - iq}\,, \tag{1}$$

where q is the center-of-mass momentum of the strongly interacting particles in the final state and δ is the corresponding (s-wave) phase shift. Close to threshold the phase shift δ can be approximated by the effective-range expansion

$$q\cot\delta = \frac{1}{a} + \frac{r_0}{2}\,q^2\,, \tag{2}$$

where for the η^3He interaction, of course, both the scattering length a and the effective range r_0 are complex.

With the above sign convention a commonly quoted necessary condition for the existence of a quasibound state is that $\Re a < 0$. However, for having a quasibound state there is an additional requirement, namely that the energy E corresponding to zero in the denominator of eq. (1) fulfils the relation $\Re E < 0$. This, in turn, implies that

$$\Re[a^3\,(a^* - r_0^*)] > 0 \tag{3}$$

in the two lowest orders in r_0/a. In the absence of the effective-range term this reduces to the condition that $|\Re a| > \Im a > 0$, given, *e.g.*, in ref. [4].

Neglecting terms of higher order than q^2, the squared reaction amplitude, $|f|^2$, can be written as [28,29]

$$\begin{aligned}|f|^2 &= |f_p|^2 \cdot |T(q)|^2 \\ &\approx \frac{|f_p|^2}{(1+\Im aq)^2 + (\Re aq)^2 + \Re a\Re r_0q^2 - \Im a\Im r_0q^2}, \end{aligned}\tag{4}$$

Table 1. Data on the reaction $p + d \to {}^3\mathrm{He} + \eta$ discussed in the present paper. q is the c.m.s. momentum in the (final) η^3He system and ε is the corresponding excess energy. We use $m_{^3\mathrm{He}} = 2809.414$ MeV and $m_\eta = 547.3$ MeV.

	Ref.	Observable	q (MeV/c)	ε (MeV)
Berger	[21]	$\sigma(0^\circ)$, $\sigma(180^\circ)$	7–136	0.054–20
Banaigs	[22]	$\sigma(180^\circ)$	265–406	73–163
Banaigs	[22]	$\sigma(\vartheta)$	283	83
Berthet	[23]	$\sigma(180^\circ)$	118–955	15–711
Mayer	[24]	σ_{tot}, $A_{\mathrm{c.m.}}$	11–75	0.13–6.11
Bilger	[25]	σ_{tot}, $\sigma(\vartheta)$	138–334	21–114
Betigeri	[26]	σ_{tot}, $\sigma(\vartheta)$	214	49
Kirchner	[27]	σ_{tot}, $\sigma(\vartheta)$	568	298

where f_p is the s-wave production operator, assumed to be independent of the final momentum near the reaction threshold.

While the coefficient of the term linear in q is given by the imaginary part of the scattering length alone, the q^2-term contains *both the complex scattering length and effective range*. In case of the two-nucleon system $|a| \gg r_0$ and therefore a further approximation is reasonable. It consists in the neglect of the effective range, *i.e.* of the second term in eq. (2), so that the reaction amplitude is simply given by

$$f = \frac{f_p}{1 - iaq}\,. \tag{5}$$

Then eq. (4) reduces to the form

$$|f|^2 = \frac{|f_p|^2}{1 + 2\Im aq + |a|^2q^2}\,. \tag{6}$$

However, for the η^3He system a and r_0 are expected to be of the same order of magnitude so that the above approximation is not really justified. Thus, here $|a|^2$ as determined from eq. (6) can only be considered as an effective quantity rather than the modulus of the physical scattering length. Clearly separating the scattering length and effective range is only possible by making further assumptions or within specific model calculations, which means in a model-dependent way. On the other hand, in the region very close to threshold where the term linear in q should dominate, in principle, there is a possibility to determine the imaginary part of the scattering length from the momentum dependence of the reaction amplitude $f(q)$. It should be feasible in the momentum range $q \leq 1/2a$.

3 Data at low energies

General information on the database discussed in the present paper is summarized in table 1.

The application of the formalism described in the previous section is only sensible if two requirements are fulfilled: i) the production data show a significant momentum dependence near threshold; ii) the production occurs predominantly in s-waves. A strong momentum dependence

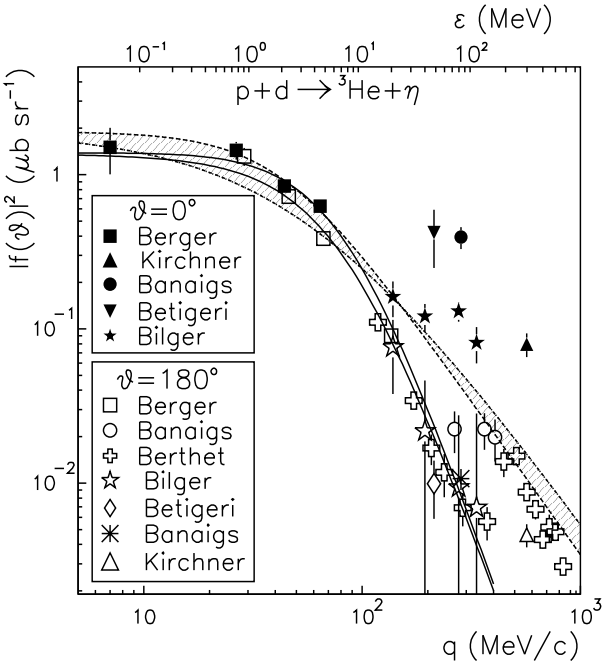

Fig. 1. Spin-averaged $p+d \to {}^3\mathrm{He}+\eta$ transition amplitude for forward (solid symbols) and backward (open symbols) η-meson production as a function of the final momentum q in the c.m. system (lower axis) or excess energy ϵ (upper axis). The experiments are taken from refs. [21–23]. In some cases [22,25–27] extrapolated results from a fit to the measured η-meson angular spectra are shown, cf. text. The solid lines are the fits of ref. [21] to their $p+d \to {}^3\mathrm{He}+\eta$ data by eq. (9) for $\vartheta = 0°$ and $\vartheta = 180°$. The shaded area indicates results based on the correlation eq. (10) reported in ref. [33] for the extreme limits given by $\Re a = 0$ and $\Im a = 0$. Here $|f|^2$ was obtained by using eq. (6).

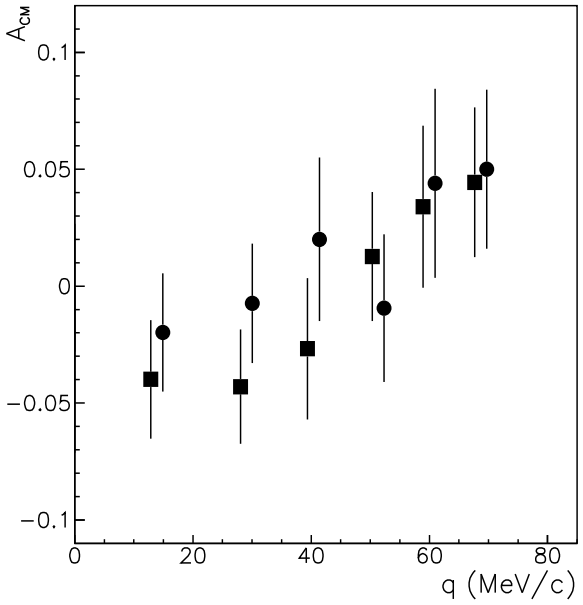

Fig. 2. Data on the η-meson forward-backward asymmetry $A_{\mathrm{c.m.}}$ as a function of final momentum q from ref. [24]. The different symbols show the experimental results obtained for different analyzing criteria [24].

of the spin-averaged squared $p + d \to {}^3\mathrm{He} + \eta$ reaction amplitude defined as

$$|f(\vartheta)|^2 := \frac{k}{q}\,\frac{\mathrm{d}\sigma}{\mathrm{d}\Omega}\,, \tag{7}$$

was indeed seen in the first reported near-threshold measurement in 1988 [21]. Here k and q are the initial and final particle momenta in the center-of-mass system and $\mathrm{d}\sigma/\mathrm{d}\Omega$ stands for the c.m.s. differential cross-section. The measurements were done only at the η-meson production angles $\vartheta = 0°$ and $\vartheta = 180°$ in the c.m.s. and are presented in fig. 1 by full and open squares. The open circles (open crosses) in fig. 1 show earlier data of Banaigs *et al.* [22] (Berthet *et al.* [23]) for η-meson production at $\vartheta = 180°$ at somewhat higher energies.

Despite the discrepancies between the data [22,23] on backward η-meson production in the range $250 \le q \le 500$ MeV/c it is clear from fig. 1 that there is a strong q-dependence of $|f(\vartheta)|^2$ up to rather high energies. Furthermore, from the data of Berger *et al.* [21], which are available for both $\vartheta = 0°$ and $\vartheta = 180°$, one can conclude that the angular dependence is small for final momenta up to $q \approx 65$ MeV/c, which suggests that the reaction amplitude should be dominated by the s-wave in this momentum range.

Further data on the reaction $p + d \to {}^3\mathrm{He} + \eta$ near threshold, obtained with the SPES2 spectrometer at Saclay, were reported in 1996 [24]. This experiment provided data on the total reaction cross-section σ_{tot} and a forward-backward asymmetry in the c.m. system $A_{\mathrm{c.m.}}$ defined as

$$\frac{\mathrm{d}\sigma}{\mathrm{d}\Omega} = \frac{\sigma_{\mathrm{tot}}}{4\pi}[1 + A_{\mathrm{c.m.}} \cos\vartheta]\ . \tag{8}$$

The latter observable is shown in fig. 2 as a function of the final momentum. The full circles and squares indicate experimental results obtained under different criteria for data analysis. Evidently, within a 5% accuracy in the amplitude the asymmetry is consistent with zero. Thus, this measurement confirms that for $q \le 70$ MeV the reaction $p + d \to {}^3\mathrm{He} + \eta$ is dominated by the s-wave. Therefore, we will use the data on $p+d \to {}^3\mathrm{He}+\eta$ in this momentum range for investigating effects of the final-state interaction (FSI) for the η^3He system.

Assuming that the total reaction cross-section is governed by the s-wave, one can compute the average reaction amplitude squared, $|f|^2$, from the data of ref. [24] by means of eq. (7). Corresponding results (now for the spin- and angle-averaged reaction amplitude) are shown in fig. 3. This figure contains also available data [30–32] for the reaction $p + d \to {}^3\mathrm{He} + \pi^0$. They are shown here in order to illustrate the strong momentum dependence of the η^3He channel, which is due to the corresponding FSI.

4 The η^3He scattering length

Berger *et al.* [21] did not attempt to extract the η^3He scattering length from their data. However, they fitted

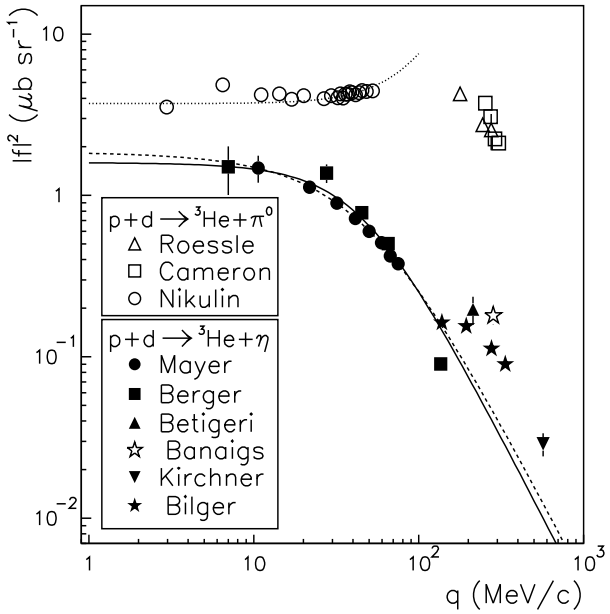

Fig. 3. Spin- and angle-averaged transition amplitudes $|f|^2$ extracted from $p+d \to {}^3\mathrm{He}+\pi^0$ [30–32] and $p+d \to {}^3\mathrm{He}+\eta$ [21, 22,24–27] data on total reaction cross-sections as functions of the final momentum q in the c.m. system. The dotted line shows the fit to the reaction $p+d \to {}^3\mathrm{He}+\pi^0$ from ref. [30]. The solid line is our overall fit by eq. (5) to low-energy data published by Mayer *et al.* [24] and Berger *et al.* [21], while the dashed line shows our fit to the data from Mayer *et al.* [24] alone.

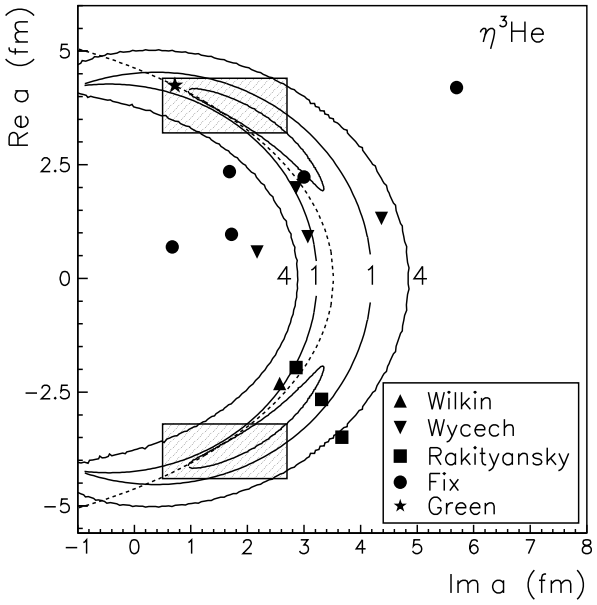

Fig. 4. Real *versus* imaginary part of the η^3He scattering length. The shaded boxes indicate the value given by Mayer *et al.* [24]. The solid contour lines show the result of our fit to the data of Mayer *et al.* [24] for $\chi^2+0.5$, χ^2+1 and χ^2+4 confidence levels, respectively. The dashed line is the parameterization of eq. (10) from ref. [33]. The symbols show results of various model calculations, taken from refs. [5] (inverse triangles), [8] (squares), [9] (circles), [33] (triangle) and [35] (star).

the data with the function

$$|f|^2 = \frac{x}{(1-yq\cos\vartheta+zq^2)^2}\ . \qquad (9)$$

The corresponding results are shown by solid lines in fig. 1 for $\cos\vartheta = \pm 1$. Note that eq. (9) is not the FSI correction to the production amplitude that follows from the Watson-Migdal approximation [28,29]. However, it can be matched to eq. (6) to order q^2 after averaging over the angle dependence. The explicit value for the modulus of the scattering length extracted in this way amounts to $|a| = 3.4 \pm 0.1$ fm, using only the errors given in ref. [21].

Employing eq. (6) Wilkin [33] analysed the preliminary Saclay data on the $p+d \to {}^3\mathrm{He}+\eta$ total cross-section [34]. He reported a correlation between the real and imaginary parts of the η^3He scattering length in the form

$$(\Re a)^2 = 21.44 - 0.449(\Im a)^2 - 4.509\Im a, \qquad (10)$$

as outcome of a χ^2 minimization. This correlation is shown in fig. 4 by the dashed line. Note that eq. (10) does not contain information about the standard χ^2+1 uncertainty of the fit and, because of the unitarity condition, it should be applied only for $\Im a \geq 0$.

We took the η^3He scattering lengths constrained by eq. (10) and employed eq. (6) to calculate the average squared reaction amplitude as a function of the final momentum. Corresponding results are shown in fig. 1, where the shaded area indicates the spread of $|f|^2$ with the limiting scattering lengths $a \simeq 0 + i3.51$ fm and $a \simeq 4.63 + i0$ fm as given in eq. (10). It is worth mentioning that Wilkin did not include the data of Berger *et al.*in his fit, though they were already available.

Mayer *et al.*used also only their own data [24] when they extracted the η^3He scattering length by utilizing eq. (5). Their result,

$$a = |3.8 \pm 0.6| + i(1.6 \pm 1.1)\ \mathrm{fm}\ , \qquad (11)$$

is shown in fig. 4 by the shaded boxes. Since, as mentioned, the sign of the real part of the η^3He scattering length cannot be inferred from a fit to the cross-section data alone, we include here boxes corresponding to $\pm\Re a$, with a given by eq. (11).

The symbols in fig. 4 represent results of various model calculations [5,8,9,33,35] based on different approaches and different elementary ηN amplitudes. For convenience, selected results are also listed in table 2 together with the elementary ηN scattering length that is employed in those model calculations. Evidently, only the result from ref. [35] is in agreement with the η^3He scattering length extracted by Mayer *et al.* [24]. In the course of our study we have refitted the data from ref. [24]. Our result is indicated by the solid contour lines in fig. 4 for $\chi^2+0.5$, χ^2+1 and χ^2+4 confidence levels. Apparently, it differs somewhat from the one published in ref. [24]. Specifically, one can see that the error correlation matrix is not symmetric and that now several model predictions from the refs. [33,5,8, 9,35] lie within the χ^2+1 confidence level.

Table 2. Model calculations of the η^3He scattering length that lie within the χ^2+1 confidence level in fig. 4. The employed values of the ηN scattering length and the used approach is also specified.

Ref.	$a(\eta^3\mathrm{He})$ (fm)	$a(\eta N)$ (fm)	Comment
[5]	$1.99+i2.86$	$0.48+i0.28$	Multiple scattering
[5]	$0.92+i3.07$	$0.43+i0.39$	Multiple scattering
[8]	$-1.96+i2.86$	$0.62+i0.30$	Finite-rank approx.
[8]	$-2.66+i3.31$	$0.67+i0.30$	Finite-rank approx.
[9]	$2.23+i3.00$	$0.57+i0.39$	Faddeev-Yakubovsky
[33]	$-2.31+i2.57$	$0.55+i0.30$	Optical potential

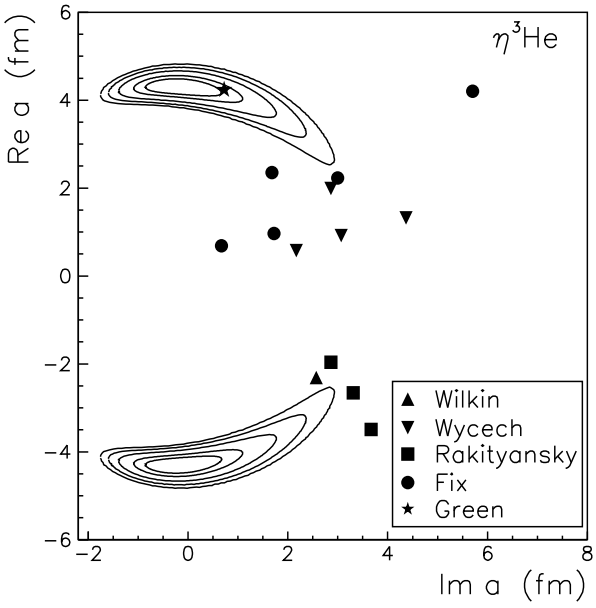

Fig. 5. Real *versus* imaginary part of the η^3He scattering length. The solid contour lines show the result of our fit to the combined data of Mayer *et al.* [24] and Berger *et al.* [21] for χ^2+0.5, χ^2+1 and χ^2+4 confidence levels, respectively. The symbols show results of various model calculations, taken from refs. [5] (inverse triangles), [8] (squares), [9] (circles), [33] (triangle) and [35] (star).

We want to point out in this context that the value of the total χ^2 at the minimum that results from our fit is $\chi^2=0.16$, which we find to be much too low. Indeed for a statistically uncorrelated set of data points one would expect a value of $\chi^2=N_{\mathrm{d.f.}}\pm\sqrt{2N_{\mathrm{d.f.}}}$, where $N_{\mathrm{d.f.}}$ is the number of degrees of freedom [36] —which in this particular case would be 5. The error bars of the Saclay data are dominated by the statistical error [24] and, therefore, they cannot be the origin of this small χ^2. Rather it seems to us that the published data points are simply not independent.

Considering this certainly to some extent strange feature of the Saclay data, one might *a priori* expect that an evaluation of the η^3He scattering length from a combined data analysis is very uncertain. Nevertheless we combine the data from Mayer *et al.* [24] and Berger *et al.* [21] to fit them by eq. (5). Corresponding results are presented

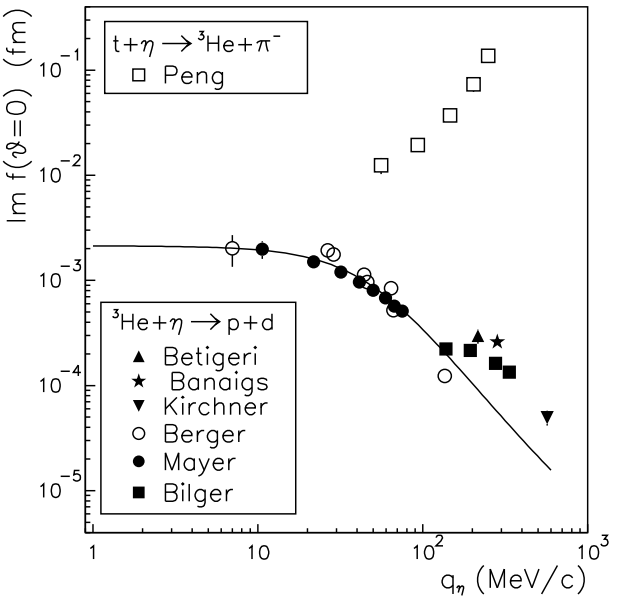

Fig. 6. Bounds on the imaginary part of the η^3He forward scattering amplitude extracted from experimental results available for the $p+d\to{}^3\mathrm{He}+\eta$ [21,22,24–27] and $\pi^-+{}^3\mathrm{He}\to t+\eta$ [37, 38] reactions. The solid line shows our estimate based on an overall fit to low-energy $p+d\to{}^3\mathrm{He}+\eta$ data.

in figs. 3 and 5. Besides yielding a substantially larger total $\chi^2=57$ also the confidence contours are different for the combined fit, as can be seen by comparing fig. 5 with fig. 4. (We show again the correlation between the real and imaginary part of the η^3He scattering length for the $\chi^2+0.5$, χ^2+1, χ^2+2, χ^2+3 and χ^2+4 confidence levels.) Obviously, the combined analysis allows for a more definite determination of the η^3He scattering length. In particular now the model predictions [5,8,9,33] lie outside of the χ^2+1 confidence level, except of the most recent result from ref. [35]. On the other hand, the fact that the resulting χ^2 minimum points to a η^3He scattering length with vanishing (or even slightly negative) imaginary part is definitely a reason to worry and is presumably a signal that the near-threshold database is internally inconsistent and/or afflicted with errors. Evidently, for further progress in the determination of the η^3He scattering length new measurements at final momenta $q<100$ MeV/c are required.

5 Estimates for the imaginary part of the scattering length

In principle, the imaginary part of the η^3He scattering length could be obtained from the total η^3+He interaction cross-section σ_{tot} by utilizing the optical theorem in the limit $q\to 0$:

$$\Im a=\lim_{q\to 0}\Im f_{\mathrm{tot}}(\vartheta=0^\circ)=\lim_{q\to 0}\frac{q}{4\pi}\,\sigma_{\mathrm{tot}}\ . \qquad (12)$$

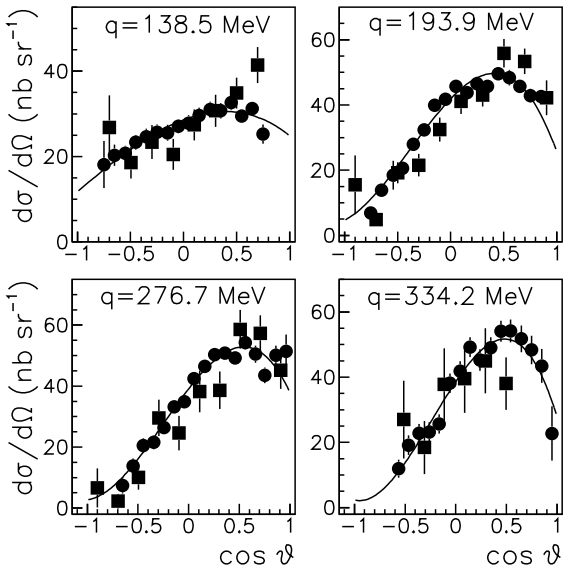

Fig. 7. Angular spectra of η-mesons produced in the $p+d \to {}^3\mathrm{He}+\eta$ reaction at different final momenta q. The data are from ref. [25] where different symbols show results obtained with different analyzing criteria. The solid lines indicate the fit given in ref. [25].

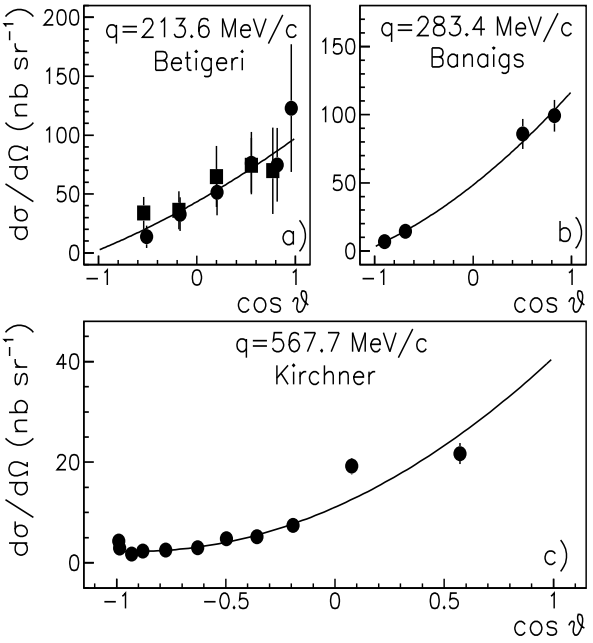

Fig. 8. Angular spectra of η-mesons produced in the reaction $p+d \to {}^3\mathrm{He}+\eta$ at different final momenta q. The data are from refs. [22,26,27]. The different symbols in a) show results obtained with different analyzing criteria [26]. The solid lines indicate our fit.

Although σ_{tot} is not accessible experimentally, one can use at least experimental information on partial $\eta^3+\mathrm{He}$ reaction cross-sections in order to deduce lower bounds on $\Im a$. This procedure works very well for the ηN case where the magnitude of the imaginary part of the scattering length is strongly constrained by the data on the $\pi^- p \to \eta n$ transition cross-section [33,17].

Using detailed balance, the $\eta^3+\mathrm{He} \to p+d$ cross-section can be related to the data available for the inverse reaction by

$$\sigma(\eta+{}^3\mathrm{He} \to p+d) = \frac{3k^2}{q^2}\,\sigma(p+d \to {}^3\mathrm{He}+\eta)\ . \quad (13)$$

In fig. 6 we show $\Im f(\vartheta=0^\circ)$ obtained via eqs. (12) and (13) from experimental results [24,21,22,25–27] available for the reaction $p+d \to {}^3\mathrm{He}+\eta$. The solid line in fig. 6 shows the estimate based on our overall fit to the low-energy data published by Mayer *et al.* [24] and Berger *et al.* [21].

One can also evaluate the partial cross-sections for $\eta+{}^3\mathrm{He} \to {}^3\mathrm{He}+\pi^0$ and $\eta+{}^3\mathrm{He} \to t+\pi^+$ from the data available for the reaction $\pi^-+{}^3\mathrm{He} \to t+\eta$ [37,38]. Taking into account the isotopical relations between the different reaction channels given by

$$\begin{aligned}\sigma(\eta+t \to {}^3\mathrm{He}+\pi^-) &= \sigma(\eta+{}^3\mathrm{He} \to t+\pi^+)\\ &= 2\sigma(\eta+{}^3\mathrm{He} \to {}^3\mathrm{He}+\pi^0)\,, \quad (14)\end{aligned}$$

the corresponding value of $\Im f(\vartheta=0^\circ)$ can be estimated. It is also included in fig. 6.

Unfortunately, the lower bounds for the imaginary part of the η^3He scattering length extracted from those reaction channels turn out to be rather small, *i.e.* $\Im a >$ 10^{-2} fm, and, therefore, are not very useful. Presumably the bulk of the inelastic cross-section comes from the reaction $\eta+{}^3\mathrm{He} \to ppn$ which is, of course, not accessible experimentally. In any case, intuitively one would expect that $\Im a$ should be at least 3 times the imaginary part of the elementary ηN scattering length. Indeed all results of microscopic calculations in the literature [5–9] (cf. also table 2) seem to be consistent with this hypothesis. Then, based on the lower bound, $\Im a_{\eta N} \approx 0.28$ fm, estimated by using the optical theorem [33] one would arrive at $\Im a \geq 0.84$ fm which might be a reasonable guess.

6 Data at higher energies

Angular spectra for the reaction $p+d \to {}^3\mathrm{He}+\eta$ at momenta $q >$100 MeV/c [25,26,22,27] are shown in figs. 7 and 8. These data exhibit already a strong asymmetry. Thus, it is clear that in this energy region the reaction is dominated by higher partial waves. Note that the solid lines in fig. 7 are taken from the original work while the curves in fig. 8 show our own fit to the experimental results using Legendre polynomials.

From those fits one can again compute the squared spin- and angle-averaged transition amplitude and the corresponding results are included in fig. 3. One can also extrapolate $|f|^2$ to very forward and backward angles and the corresponding values are shown in fig. 1. We detect substantial discrepancies between the $p+d \to {}^3\mathrm{He}+\eta$ forward cross-sections extrapolated from the data of Bilger *et al.* [25], Banaigs *et al.* [22] and Betigeri *et al.* [26]. The

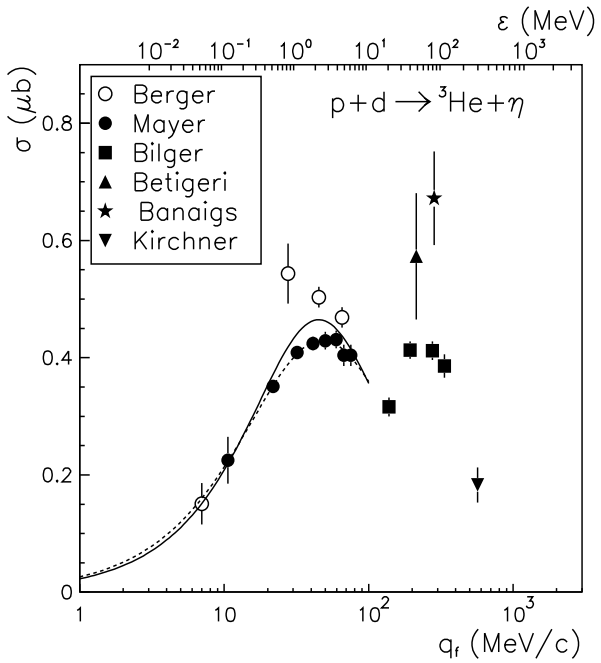

Fig. 9. The $p + d \rightarrow {}^3\mathrm{He} + \eta$ total reaction cross-section as a function of the final momentum q in the c.m. system (lower axis) or excess energy ϵ (upper axis). The data are from refs. [21,22,24–27]. The solid line is our overall fit by eq. (5) to low-energy data published by Mayer *et al.* [24] and Berger *et al.* [21], while the dashed line shows our fit to the data from Mayer *et al.* [24] alone.

extrapolated data on backward η-meson production [25, 26,22,27] are in rough agreement with other published results [21,23] for $q < 300$ MeV/c, taking into account that the data from ref. [25] have large uncertainties.

The discrepancies between the available data are also reflected in fig. 9, where the experimental results [21,22, 24–27] on the $p + d \rightarrow {}^3\mathrm{He} + \eta$ total reaction cross-section are shown as a function of the final momentum q in the c.m. system and the excess energy ϵ. Here with open circles we also present total reaction cross-sections for the data of Berger *et al.* [21], derived from their forward and backward η-meson production cross-sections via eq. (8). Evidently, there is not much consistency between the various data sets —neither for low nor for higher energies.

7 Summary

We have critically reviewed the presently available data for the reaction $p + d \rightarrow {}^3\mathrm{He} + \eta$ with the aim of extracting the η^3He scattering length. The experimental information on angular spectra clearly shows that the reaction is dominated by the s-wave up to final momenta of around 70 MeV/c and, therefore, we have used all data in this energy range for the evaluation of the η^3He scattering length.

The analysis provides strong indications that the low-energy data published by Berger *et al* [21] and Mayer *et al.* [24] are not consistent with each other. The overall fit to all low-energy data [21,24] results in a large total χ^2 of 57, however clearly locates the scattering length as $\Im a = 0.5 \pm 0.5$ fm and $\Re a = 4.3 \pm 0.3$ fm. The fit to the data from Mayer *et al.* [24] alone results in a rather small total χ^2 of only 0.16, but yields an η^3He scattering length with much too large statistical uncertainty.

Further progress in the determination of the η^3He scattering length requires new measurements at final momenta $q \leq 70$ MeV/c in order to settle the ambiguities exhibited by the present database. In particular, it would be nice to obtain information about the $p + d \rightarrow {}^3\mathrm{He} + \eta$ reaction cross-section very close to threshold, because this would provide us with more stringent constraints for the imaginary part of the scattering length. Furthermore, measurements of the angular spectrum of the η-meson at energies corresponding to final momenta around $q = 70$ MeV/c would be very useful. Such data would allow to examine whether the reaction is still dominated by the s-wave up to this energy —as we assumed in our analysis. The mentioned experiments could be done at accelerator facilities like COSY and CELSIUS [13,39].

Our systematical analysis shows that the $p+d \rightarrow {}^3\mathrm{He}+\eta$ data available at larger final momenta, $q >100$ MeV/c, are also not consistent with each other. Obviously this situation constitutes a substantial difficulty in the comparison between the experimental results and theoretical calculations. Here, too, the problem can be solved only by improving and expanding the database for the reaction $p + d \rightarrow {}^3\mathrm{He} + \eta$.

This work was performed in part under the contract No. DE-FG02-93ER40756 with the University of Helsinki. Financial support for this work was also provided in part by the international exchange program between DAAD (Germany, Project No. 313-SF-PPP-8) and the Academy of Finland (Project Nos. 41926 and 54038).

References

1. Q. Haider, L.C. Liu, Phys. Lett. B **172**, 257 (1986).
2. L.C. Liu, Q. Haider, Phys. Rev. C **34**, 1845 (1986).
3. H.C. Chiang, E. Oset, L.C. Liu, Phys. Rev. C **44**, 738 (1991).
4. Q. Haider, L.C. Liu, Phys. Rev. C **66**, 045208 (2002).
5. S. Wycech, A.M. Green, J.A. Niskanen, Phys. Rev. C **52**, 544 (1995).
6. S.A. Rakityansky, S.A. Sofianos, W. Sandhas, V.B. Belyaev, Phys. Lett. B **359**, 33 (1995).
7. V.B. Belyaev, S.A. Rakityansky, S.A. Sofianos, M. Braun, W. Sandhas, Few-Body. Syst. Suppl. **8**, 309 (1995).
8. S.A. Rakityansky, S.A. Sofianos, M. Braun, V.B. Belyaev, W. Sandhas, Phys. Rev. C **53**, R2043 (1996).
9. A. Fix, H. Arenhövel, Phys. Rev. C **66**, 024002 (2002).
10. R.S. Hayano *et al.*, GSI/SIS Proposal S214 (1997).
11. R.S. Hayano, S. Hirenzaki, A. Gillitzer, Eur. Phys. J. A **6**, 99 (1999).
12. H. Machner *et al.*, COSY Proposal No. 50.1 (2000).
13. A. Khoukaz *et al.*, COSY Proposal No. 62.2 (2000).
14. A. Gillitzer *et al.*, COSY Proposal No. 102 (2001).

15. P. Grassberger, W. Sandhas, Nucl. Phys. B **2**, 181 (1967); E.O. Alt, P. Grassberger, W. Sandhas, Phys. Rev. C **1**, 85 (1970).
16. O.A. Yakubovsky, Sov. J. Nucl. Phys. **5**, 937 (1967).
17. A. Sibirtsev, S. Schneider, Ch. Elster, J. Haidenbauer, S. Krewald, J. Speth, Phys. Rev. C **65**, 044007 (2002).
18. R.G. Newton, *Scattering Theory of Waves and Particles* (Springer-Verlag, New York, 1982).
19. M. Goldberger, K.M. Watson, *Collision Theory* (Wiley, New York, 1964).
20. V. Baru, J. Haidenbauer, C. Hanhart, J.A. Niskanen, Phys. Rev. C **68**, 035203 (2003).
21. J. Berger *et al.*, Phys. Rev. Lett. **61**, 919 (1988).
22. J. Banaigs *et al.*, Phys. Lett. B **45**, 394 (1973).
23. P. Berthet *et al.*, Nucl. Phys. A **443**, 589 (1985).
24. B. Mayer *et al.*, Phys. Rev. C **53**, 2068 (1996).
25. R. Bilger *et al.*, Phys. Rev. C **65**, 044608 (2002).
26. M. Betigeri *et al.*, Phys. Lett. B **472**, 267 (2000).
27. T. Kirchner, PhD Thesis, Institute de Physique Nucleaire, Orsay (1993).
28. K.M. Watson, Phys. Rev. **88**, 1163 (1952).
29. A.B. Migdal, Sov. Phys. JETP **1**, 2 (1955).
30. V.N. Nikulin *et al.*, Phys. Rev. C **54**, 1732 (1996).
31. J.M. Cameron *et al.*, Nucl. Phys. A **472**, 718 (1987).
32. E. Roessle *et al.*, *Proceedings of the Conference on Pion Production and Absorption in Nuclei*, AIP Conf. Proc. **79**, 171 (1982).
33. C. Wilkin, Phys. Rev. C. **47**, R938 (1993).
34. R. Kessler, PhD Thesis, UCLA (1992).
35. A.M. Green, S. Wycech, Phys. Rev. C **68**, 061601 (2003).
36. J.R. Bergervoet, P.C. van Campen, W.A. van der Sanden, J.J. de Swart, Phys. Rev. C **38**, 15 (1988).
37. J.C. Peng *et al.*, Phys. Rev. Lett. **58**, 2027 (1987).
38. J.C. Peng *et al.*, Phys. Rev. Lett. **63**, 2353 (1989).
39. A. Khoukaz *et al.*, in preparation.